Atomic Surface Structure of UHV-Prepared Template-Stripped Platinum and Single-Crystal Platinum(111)

ARTICLE *in* THE JOURNAL OF PHYSICAL CHEMISTRY B · DECEMBER 2004

Impact Factor: 3.3 · DOI: 10.1021/jp0466789

5 AUTHORS, INCLUDING:

Regina Ragan
University of California, Irvine
64 PUBLICATIONS **542** CITATIONS

SEE PROFILE

Stan Williams
Hewlett-Packard
510 PUBLICATIONS **22,436** CITATIONS

SEE PROFILE

Atomic Surface Structure of UHV-Prepared Template-Stripped Platinum and Single-Crystal Platinum(111)

Regina Ragan,*,†,‡,# Doug Ohlberg,†,# Jason J. Blackstock,*,†,§,# Sehun Kim,†,|| and R. Stanley Williams†

Quantum Science Research Group, Hewlett-Packard Laboratories, 1501 Page Mill Road, MS 1123, Palo Alto, California 94304, Department of Physics, Avadh Bhatia Physics Laboratory, University of Alberta, Edmonton, AB, T6G 2J1, Canada, and Department of Chemistry, Korea Advanced Institute of Science and Technology, 373-1 Guseong-dong, Yuseong-gu, Daejeon, 305-701, Korea

Received: July 26, 2004; In Final Form: September 24, 2004

A novel method is presented for preparing ultraflat noble metal surfaces in situ under ultrahigh vacuum from thin metal films that are deposited via physical vapor deposition on commercially available silicon substrates. The method, based on template stripping of thin metal films from Si wafer surfaces, is utilized in this paper to prepare atomically smooth, uncontaminated platinum surfaces for examination by scanning-tunneling microscopy under ultrahigh vacuum conditions. As a standard for comparison, single-crystal Pt(111) surfaces are also examined. The resulting scanning-tunneling microscopy data clearly demonstrate that under the surface preparation conditions examined here, template-stripped platinum surfaces are predominantly ⟨111⟩ textured with a surface roughness equivalent to or better than a single-crystal Pt(111) surface.

Introduction

Studies of self-assembled monolayers (SAMs) on metal surfaces have shown that the roughness of the underlying substrate surface has considerable influence on the quality of the molecular film.[1−7] Since the first demonstration of template stripping over a decade ago,[8] template-stripped (TS) surfaces (particularly Au) have been increasingly used as substrates for SAMs of organic molecules[9−12] and biomolecules[13,14] due to their exceptional flatness, ease of fabrication, and low unit cost as compared to single-crystal substrates. Although a variety of surface characterization techniques have been applied to various TS surfaces, including scanning probe microscopy[4,8,9,15] and X-ray diffraction,[15] there has been very little work on the atomic structure of these surfaces. Yet, the atomic surface structure of the underlying substrate is an extremely important factor in SAM growth[16,17]—at the very least, equal in importance to surface roughness. STM studies of alkanethiol SAMs on single-crystal Au(111)[18,19] and Pt (111)[20] demonstrate that the SAM initially adopts the hexagonal symmetry of the substrate. The molecular arrangement of the alkanethiol monolayer on Au(111) forms a $c(4 \times 2)$ superlattice with $\sqrt{3} \times \sqrt{3}$ R30° hexagonal lattice.[18] An understanding of the atomic arrangement or surface reconstruction of the metal surface is thereby essential to an understanding of the SAM overlayer.

To the best of our knowledge, only one publication, to date, has claimed to observe atomically resolved surface structure of an annealed Au TS film that was stripped from mica.[9] Wagner et al.[9] state that they imaged Au atoms arranged in the close-packed face-centered-cubic (fcc) lattice with the surface normal oriented along the [111] direction using ambient condition scanning-tunneling microscopy (STM). However, no images were reproduced in the publication. Despite the many advantages of TS substrates—including exceptional flatness, purity, and ease of fabrication and handling—in order for TS films to be employed in fundamental studies and advanced applications of SAMs, a method for clearly and routinely elucidating the atomic surface structure of TS substrates must be available.

Surface characterization methods such as STM, Auger electron spectroscopy, low-energy electron diffraction, and other techniques that have a penetration depth of a few monolayers provide information regarding atomic-scale defects, chemical composition, and atomic periodicity of surfaces. These techniques are also highly sensitive to surface contamination however, which can obscure surface structure and complicate analysis. Despite the pristine cleanliness of freshly stripped TS surfaces,[15] TS samples that are stripped under ambient conditions will immediately accumulate considerable adsorbates within the minutes required to load them into UHV systems for analysis in an environment free from the ongoing contamination of the ambient. This has been observed on platinum surfaces where the accumulation of contaminants was monitored by measuring the changes in contact angle and index of refraction over time following exposure to air.[21] In most cases, a sample is simply loaded from the lab environment with the accumulated surface adsorbates and contaminants into a UHV system. The sample is then baked and annealed in order to remove contaminants from the sample holder and substrate surface and sometimes sputter-cleaned with an Ar ion beam to generate a clean surface. Unfortunately, such a cleaning procedure is incompatible with TS samples, as the epoxy used in the process cannot withstand high annealing temperatures and the original templated surface structure would be lost in the annealing and sputtering steps.

To overcome these challenges, we developed a TS sample geometry and in-situ stripping method that allows TS surfaces to remain protected by the templating surface until after the sample is loaded into the UHV system. Once in UHV, the TS

# These three authors contributed equally to this work.
* To whom correspondence should be addressed. R.R.: phone (949) 824-6830. e-mail rragan@uci.edu. J.J.B.: phone (780) 718-6630 (Canada) or (650) 857-2801 (U.S.); e-mail jjb@ualberta.ca or jason.blackstock@hp.com.
† Hewlett-Packard Laboratories.
‡ Currently at the University of California, Irvine.
§ University of Alberta, Edmonton.
|| Korea Advanced Institute of Science and Technology.

10.1021/jp0466789 CCC: $27.50
Published on Web 11/26/2004

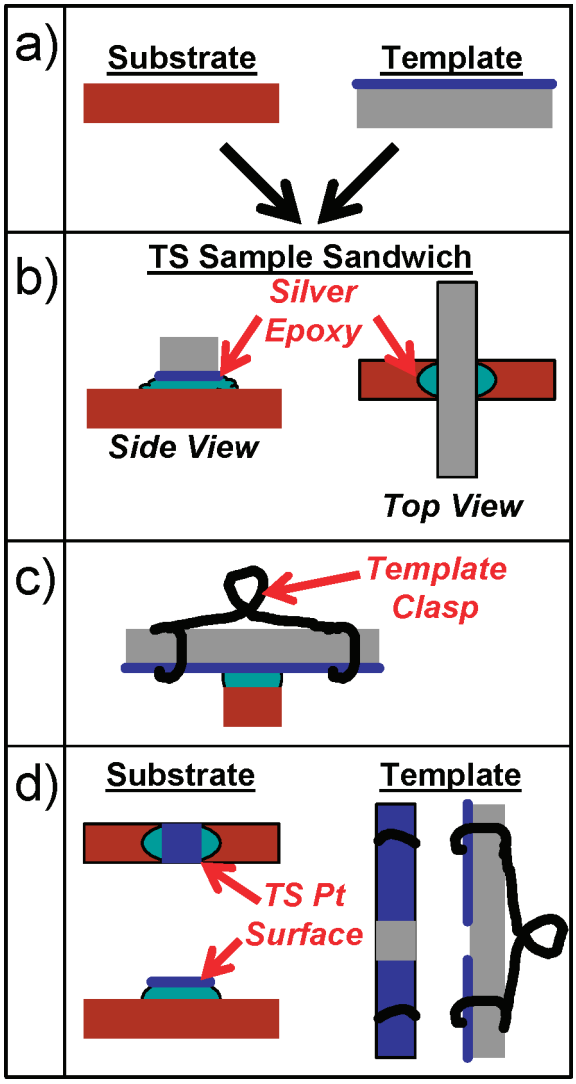

Figure 1. Schematic of the in-situ template-stripping procedure used to prepare TS−Pt samples in a UHV environment. (a) Si(001) substrate and Pt film (blue) on SiO_x/Si(001) template. (b) TS sandwich structure. (c) Template clasp that is used for removal of Si template in UHV. (d) Illustration of removal of Pt thin film from Si template and transfer to Si substrate

surfaces are annealed while still sealed to their templates, baking away contaminants from the sample holder that could later migrate to the TS surfaces. After baking, the samples are stripped in UHV, providing pristine TS surfaces for further analysis with surface specific UHV techniques.

In this paper we use our in-situ TS sample preparation procedure to produce samples of TS Pt for UHV−STM characterization, building on our previous work with TS Pt.[15] STM examinations of the TS Pt surface are conducted over length scales ranging from a few nanometers to micrometers. The atomic and nanoscale structure of TS Pt is compared with that of a single-crystal Pt(111) sample prepared by standard techniques. The results clearly demonstrate that TS Pt surfaces—prepared as described in the text—are predominantly ⟨111⟩ textured and polycrystalline, with a surface roughness equivalent to or better than a single-crystal Pt(111) surface.

Experimental Section

Template-Stripped Sample Preparation. The TS sample 'sandwiches' are prepared from two rectangular pieces of silicon, approximately 3 mm × 12 mm, as shown in Figure 1 a and b. Prior to any processing, the Si rectangles are cleaved from larger (normally 4 in.) Si wafers and cleaned in piranha solution (1:3 by volume mixture of 30% hydrogen peroxide and concentrated sulfuric acid) for 15 min. The piranha cleaning step leaves a thin oxide layer on the Si substrate.[15]

The substrate, i.e., the Si surface to which the TS Pt film is to be transferred, is cleaved from a highly doped prime Si(001) wafer (N/arsenic, ≤ 0.004 Ωcm). Immediately following the piranha clean, the Si substrate is coated with layers of Al and Pt (150 and 200 Å, respectively) at a deposition rate of 1 Å/s using an electron beam evaporator in a vacuum with a pressure of $\leq 10^{-6}$ Torr. The deposition is carried out in two stages (one for each side) with the Si substrate at a tilt of ∼45° to the incident flux. The substrate is tilted to ensure that the entire surface—front, back, and sides—is coated with a continuous metal film. The reason for encasing the entire Si substrate under Al and Pt overlayers is to reduce STM image noise that can arise from bad electrical contact between the substrate and ground.

As in our previous work with TS Pt,[15] the templates used for these experiments are p-type Si(001) substrates (P/boron, 1−20 Ωcm). Immediately after piranha cleaning the Si(001) template, Pt is deposited via an e-beam evaporator on the Si(001) substrate at normal incidence in a vacuum with a pressure of $\leq 10^{-6}$ Torr. Pt is deposited on only one side of the template, which is kept at room temperature during deposition. The evaporation rate is incrementally increased over the period of the evaporation, starting at 0.1 Å/s for the first 50 Å, 0.5 Å/s for the next 100 Å, and finally 1.0 Å/s for the remainder of the 120 nm thick film.

Following metal deposition, the rectangular faces of the substrate and template are glued to one another with silver epoxy to make a TS sample sandwich as shown in steps a and b of Figure 1. The rectangular faces are joined with their long axes orthogonal to one another. In addition to serving as an adhesive, the silver epoxy (Epo-Tek H 21D) also provides a low-resistance path for electrons through the TS surface to ground during STM experiments. The sample is subjected to a brief heat treatment at 180 °C for 10 min in an oven to cure the silver epoxy, thus completing the fabrication of the TS sample sandwiches.

In-Situ Template-Stripping Procedure. Prior to loading the samples into the UHV chamber, wires are wrapped around the ends of the Si template and spot-welded to a small wire loop that projects away from the center of the backside of the Si template, forming a clasp as shown in Figure 1c. Next, the TS sandwich is mounted in a sample holder with the Si substrate mounted face up in the sample holder, constraining the metal clasp of the now downward-facing template to extend away from the face of the sample holder. The Si template is only attached to the Si substrate and thereby the sample holder via the silver epoxy. The sample holder is then loaded into an UHV Omicron STM/AFM system with a base pressure of $\leq 10^{-10}$ Torr. Prior to in-situ stripping, the sample holder and sample were baked at 145 °C for 18 h to remove water and contaminants from the sample holder that could migrate onto the fresh TS surface after template stripping.

To carry out the process of in-situ template stripping, a wobble stick is used to grab the wire clasp on the Si template. With the Si substrate held rigidly in place by the sample holder, the wobble stick is given a gentle pull. Due to the poor adhesion of Pt to the oxide layer of the piranha-cleaned Si template, the Pt cleaves easily from the SiO_x surface in the UHV environment and remains attached to the Si substrate via the silver epoxy. As shown in Figure 1d, the fresh template-stripped Pt surface

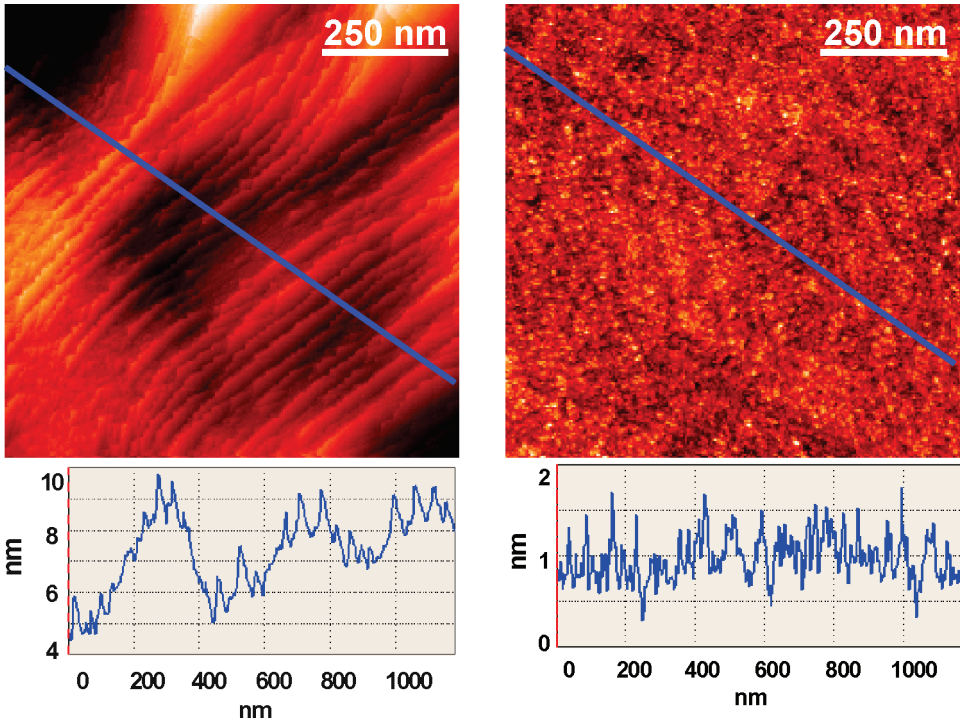

Figure 2. STM (1 μm)^2 topography images (a) SC Pt(111) taken in constant current mode with 1.66 nA and 0.58 gap voltage (V_{gap}) and (b) TS Pt taken with 0.91 nA and 1.06 V_{gap}. The blue line on the images denotes the section represented by the line profiles on the bottom of the images.

is exposed face up in the sample holder. For clarity, a demonstration of the mechanical stripping process with the wobble stick outside of the UHV chamber is shown as Figure S1 in the Supporting Information accompanying this paper.

Single-Crystal Pt(111) Surface Preparation. The single-crystal Pt(111) surface is prepared in an UHV chamber by first sputtering it at room temperature with a 1 kV, ca. 35 μA, Ar ion beam under dynamic flow conditions adjusted to maintain an Ar background pressure of 10^{-5} Torr. After sputtering, the Pt(111) sample was annealed at 800 °C in an O_2 ambient of 10^{-8} Torr. The initial sputter regime was repeated and followed by an anneal in UHV at 800 °C. This process was iterated until STM imaging verified an atomically clean Pt(111) surface.

Results

STM Analysis of Surface Features and Roughness. The freshly exposed TS Pt surface was probed by STM immediately after stripping. Shown in Figure 2 a and b are (1 μm)^2 STM images of single-crystal (SC) Pt(111) and TS Pt, respectively. Large atomically flat terraces are visible on the SC Pt(111) surface. In Figure 2a the step edges are parallel to the $\langle\bar{1}0\rangle$ direction and exhibit numerous salients with 60° angles where those sections of the step edge oriented along a $[0\bar{1}1]$ direction encounter sections oriented along a $[\bar{1}01]$ direction. Qualitatively, the TS Pt surface appears quite dissimilar to the SC Pt(111) surface on the micrometer length scale. Atomically flat terraces on the TS Pt surface are not distinguishable at this scale, whereas flat terraces are observed on the SC Pt(111) surface. Despite the lack of large terraces, TS Pt shows smaller variations in vertical topography than SC Pt(111), as evidenced by the cross-sectional profile provided at the bottom of Figure 2. Using RMS roughness as a criterion, the TS Pt surface is quantitatively smoother than SC Pt(111). The RMS roughness values of the two surfaces are 2.7 Å for TS Pt versus 29.7 Å for the SC surface.[22]

Figure 3a and b shows (50 nm)^2 STM images of both the SC Pt(111) and TS Pt surfaces, respectively, clearly revealing individual terraces and steps on both surfaces. Though large terraces are not visible on the TS Pt film at the micrometer length scale, atomically flat terraces tens of nanometers in width are observed in the higher resolution scan of Figure 3b. Qualitative differences between the two surfaces are pronounced in Figure 3. Whereas the SC Pt(111) surface demonstrates straight terrace boundaries, the terrace edges on the TS surface appear highly kinked and meandering. Although the terrace boundaries appear curved in Figure 3b, a higher resolution image taken of the region defined by the white box in Figure 3b reveals highly kinked step edges with crystal facets. Step bunching is evident on the (50 nm)^2 image of the SC Pt(111) surface, where, on average, adjacent terraces are separated by distances of multiple atomic steps—unlike the TS surface where step heights are only one or two atomic layers. The dramatic differences in RMS values calculated from the (1 μm)^2 images of SC Pt(111) and TS Pt shown in Figure 2 stem from step bunching and multilayer step heights between terraces on SC Pt(111). This is illustrated in the jagged saw-tooth like appearance of the line profile, shown below Figure 2a.

Another feature of the TS surface observable in the (100 nm)^2 STM image presented in Figure 4 is the lack of a single in-plane crystallographic orientation for neighboring Pt crystallites; the step edges on neighboring crystallites are not separated by 60° angles as expected for step edges parallel to $\langle 1\bar{1}0\rangle$ on a single-crystal surface. While both [111] textured, the left two-thirds of the image displays step edges running vertically, whereas the right one-third demonstrates horizontal step edges, indicative of two different in-plane orientations. It is hypothesized that with no preferential orientation provided by the amorphous oxide on Si(100), crystallites arrange in the lowest energy configuration—the close-packed fcc lattice—during the evaporation and annealing stages. Independently nucleated crystals have a random in-plane rotation with respect to neighboring crystals due to the absence of an energy minima for a particular in-plane orientation. On this length scale the boundaries between neighboring regions showing planar mis-

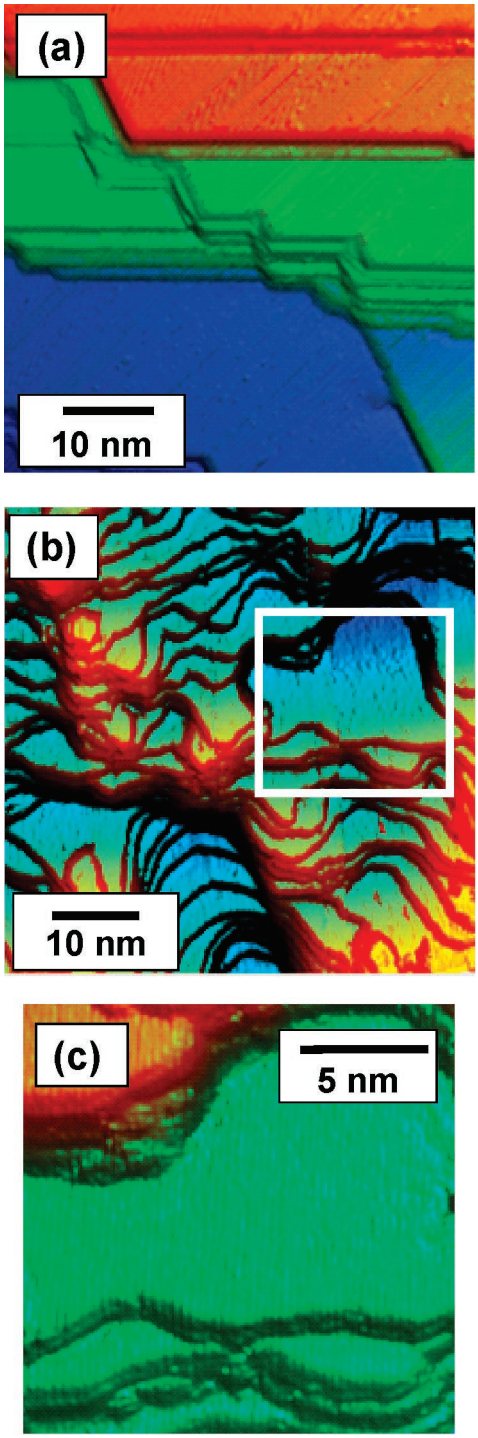

Figure 3. STM (50 nm)^2 images taken in constant current mode of (a) SC Pt(111) (-0.32 V_{gap} and 2.42 nA) and (b) TS Pt (-0.66 V_{gap} and 1.46 nA). (c) The region highlighted by white box in b shows the highly kinked step edges. The laplacian was convoluted with the original STM image for each image to accentuate local curvature.

orientation are therefore attributed to grain boundaries between neighboring crystallites at the TS surface. On the basis of this method of identifying individual Pt crystallites, the grain size of the TS Pt sample was estimated to be between 15 and 40 nm in diameter from numerous (50 nm)^2 and (100 nm)^2 STM images.

The mechanisms underlying the appearance of the small terraces and curved step edges on the TS surface are seemingly the result of the evaporative nucleation and annealing growth process by which the TS surface is formed. This process clearly

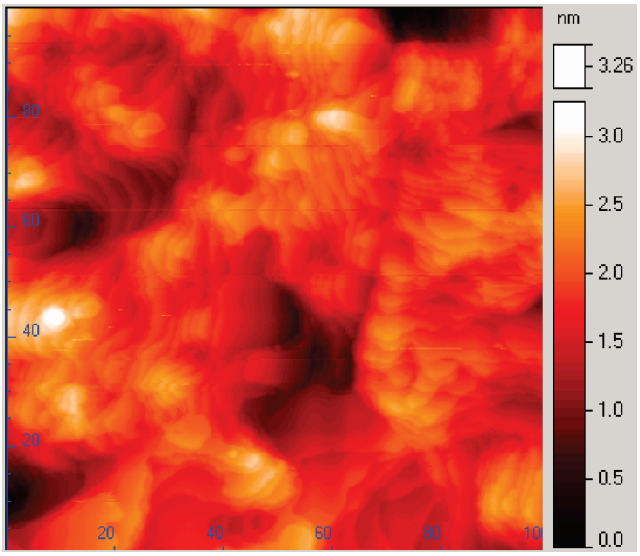

Figure 4. STM (100 nm)^2 image of a TS Pt surface demonstrating different rotational orientations of neighboring [111] textured crystallites.

includes interactions and competition between neighboring grains as well as the influence of atomic features/defects on the silicon-oxide templates. In comparison, on the SC Pt(111) surface step edges are mobile over longer distances due to the higher annealing temperature and lack of restrictive templating surface, resulting in the observed wider terraces. Pinning of step edges occurs only at infrequent impurity sites on the SC surface, thus leading to significant step bunching where impurities do occur. This accounts for the higher observed RMS roughness value of SC Pt(111) that differs from that of the TS Pt by an order of magnitude.

Although smoother surfaces of SC Pt(111) have been reported,[23] it is important to note that such surfaces are costly in terms of the material expenses associated with the single crystal and the time investment required for surface preparation. The necessity of producing a cheaper, more practical alternative with a comparable surface roughness has been underscored by recent studies of electron transport across metal/SAM/Pt polycrystalline surfaces,[24,25] which would have been prohibitively costly to conduct with SC Pt. These studies demonstrated that RMS roughness values greater than a few angstroms lead to negligible device yields.[24,25] Atomically flat surfaces that can be practically prepared are therefore critical for molecular electronic device fabrication, and the TS fabrication procedure examined here provides one simple route to obtaining such surfaces. Further investigations of TS surfaces with varied evaporation and annealing conditions will provide the opportunity to develop detailed insight into the physics-rich behavior at the platinum−silicon oxide interface and optimize the surface for SAM deposition.

Surface Orientation. From a compilation of STM images of both surfaces—on a similar length scale to those shown in Figure 3—the average value for the thickness of a single atomic layer was determined to be 2.7 ± 0.8 Å for the SC Pt(111) surface and 2.5 ± 0.2 Å for the TS surface. The quoted values are an average of at least 10 different measurements on each surface, and the quoted error is the standard deviation of the average—the larger error quoted for the SC surface is due to the fact that the majority of steps observed were multiple atomic layers in height, making quantification of the single atomic layer thickness more challenging. For reference, two examples of step

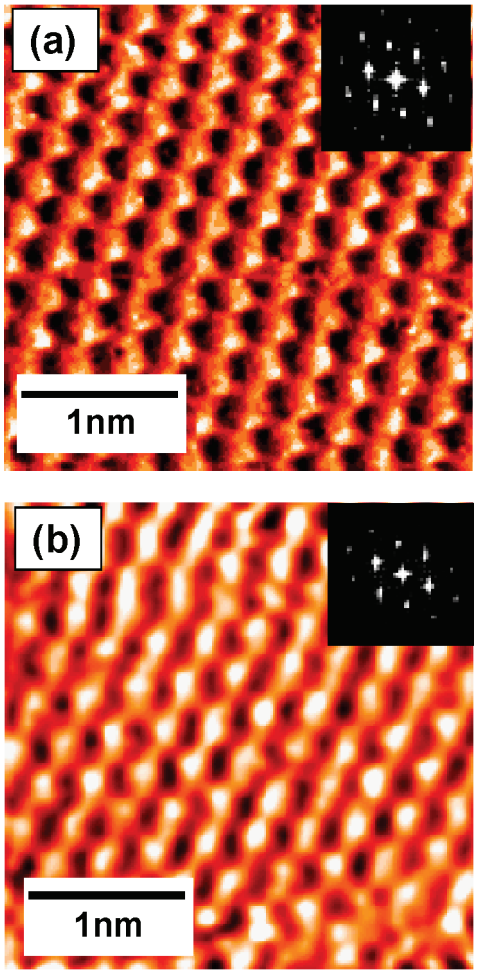

Figure 5. High-resolution (3 nm)^2 STM images taken with current feedback of (a) SC Pt(111) (−0.1 V_{gap} and 2.42 nA) and (b) TS Pt (0.45 V_{gap} and 0.85 nA). The 6-fold symmetry of the hexagonal close-packed lattice is clearly distinguishable in the images and FFT patterns shown in the insets.

height measurements for each surface are provided in Figure S2 of the Supporting Information accompanying this paper.

The measured atomic layer thicknesses of the SC Pt(111) and TS Pt samples are in good agreement, both with each other and with the value expected for the interplanar spacing between[19] planes of Pt atoms (2.25 Å) in the fcc lattice. This suggests that while the various grains of the TS Pt are randomly rotated in the plane of the surface relative to each other, they appear predominantly ⟨111⟩ vertically orientated. Atomic resolution STM images of SC Pt(111) and TS Pt surfaces taken on flat terraces are shown in Figure 5a and b, respectively, each including insets showing the fast Fourier transforms (FFTs) of the images. Both images clearly show a fcc close-packed lattice, and the reciprocal space FFT patterns demonstrate the corresponding 6-fold symmetry of the ⟨1$\bar{1}$0⟩ reflections. Quantitatively, the interatomic spacing of the surfaces was determined from the location of the first-order spots in FFT pattern, yielding values of 2.7 ± 0.3 Å for the TS surface and 2.5 ± 0.3 Å for the SC surface. Once again, the quantitative values show exceptional agreement with each other as well with the expected value of 2.8 Å for the nearest-neighbor spacing of Pt atoms in the fcc lattice. These results are also in agreement with previous X-ray diffraction measurements showing polycrystalline TS Pt films to have a bulk ⟨111⟩ orientation.[15]

Discussion and Conclusions

The STM results presented in this paper have clearly elucidated the atomic and nanoscale surface structure of TS Pt surfaces prepared as described above. In this work we have shown that TS Pt surfaces are predominantly ⟨111⟩ textured, with terrace widths on the order of 10 nm and separated in height by only a few atomic layers. As discussed in the Introduction, this level of knowledge of the surface structure is essential for detailed understanding and control of SAMs grown on TS films. Indeed, this demonstration of an in-situ UHV template-stripping procedure creates the possibility of exploring UHV vapor-phase growth of SAMs on TS Pt surfaces in addition to other metal surfaces. Further studies will compare SAM growth on TS Pt versus SC Pt(111).

Beyond elucidating the atomic structure of the TS Pt films prepared for this work, the STM results also raised tantalizing questions regarding the nucleation and growth mechanism driving the formation of the TS Pt surface. Using this in-situ UHV template-stripping technique, the parameter space of different evaporation and annealing conditions for preparing TS platinum surfaces can be explored and optimized as can be done for other TS surfaces such as silver and gold. In addition, other UHV techniques such as LEED can be performed, thus providing additional information regarding long-range atomic order and defects exhibited by these surfaces. These studies have the potential to provide tremendous insight into the nucleation and growth mechanisms of nonadhering vapor-phase-deposited thin films.

Acknowledgment. The authors thank Duncan R Stewart and Zhiyong Li (QSR, HP Labs) for their numerous fruitful discussions and gratefully acknowledge the assistance of Eric Carpenter, Dave Fortin, and Dr. Michael Horn-von Hoegen with STM data analysis (Department of Physics, University of Aberta). J.J.B. kindly thanks NSERC and iCORE for partial funding, and the authors thank DARPA for partial funding of this research. S.K. thanks the KOSEF through CNNC for partial funding.

Supporting Information Available: Pictorial overview of the UHV template-stripping procedure and examples of atomic step-height measurements. This material is available free of charge via the Internet at http://pubs.acs.org.

References and Notes

(1) Guo, L.-H.; Facci, J. S.; McLendon, G.; Mosher, R. *Langmuir* **1994**, *10*, 4588−4593.
(2) Terrill, R. H.; Tanzer, T. A.; Bohn, P. W. *Langmuir* **1998**, *14*, 845−854.
(3) Losic, D.; Shapter, J. G.; Gooding, J. J. *Langmuir* **2001**, *17*, 3307−3316.
(4) Losic, D.; Shapter, J. G.; Gooding, J. J. *Aust. J. Chem.* **2001**, *54*, 643−648.
(5) Leopold, M. C.; Black, J. A.; Bowden, E. F. *Langmuir* **2002**, *18*, 978−980.
(6) Leopold, M. C.; Bowden, E. F. *Langmuir* **2002**, *18*, 2239−2245.
(7) Yang, J.; Han, J.; Isaacson, K.; Kwok, D. Y. *Langmuir* **2003**, *19*, 9231−9238.
(8) Hegner, M.; Wagner, P.; Semenza, G. *Surf. Sci.* **1993**, *291*, 39−46.
(9) Wagner, P.; Hegner, M.; Guntherodt, H. J.; Smemnza, G. *Langmuir* **1995**, *11*, 3867−3875.
(10) Wong, S. S.; Porter, M. D. *J. Electroanal. Chem.* **2000**, *485*, 135−143.
(11) Huang, Y. W.; Gupta, V. K. *Macromolecules* **2001**, *34*, 3757−3764.
(12) Huang, Y. W.; Gupta, V. K. *Langmuir* **2002**, *18*, 2280−2287.

(13) Wagner, P.; Zaugg, F.; Kernen, P.; Hegner, M.; Semenza, G. *J. Vac. Sci. Technol., B* **1996**.
(14) Ge, C. W.; Liao, J. H.; Yu, W.; Gu, N. *Biosens. Bioelectron.* **2003**, *18*, 53−58.
(15) Blackstock, J. J.; Li, Z.; Freeman, M. R.; Stewart, D. R. *Surf. Sci.* **2003**, *546*, 87−96.
(16) Ulman, A. *Chem. Rev.* **1996**, *96*, 1533−1554.
(17) Schwartz, D. K. *Annu. Rev. Phys. Chem.* **2001**, *52*, 107−137.
(18) Poirier, G. E. *Chem. Rev.* **1997**, *97*, 1117.
(19) Noh, J.; Hara, M. *Langmuir* **2001**, *18*, 1953.
(20) Ragan, R.; Kim, S.; Ohlberg, D. A. A.; Williams, R. S. Unpublished results.
(21) Li, Z.; Beck, P.; Ohlberg, D. A. A.; Stewart, D. R.; Williams, R. S. *Surf. Sci.* **2003**, *529*, 410.
(22) The RMS surface roughness of the TS Pt surface quoted here is slightly higher than that previously observed for similar surfaces. This is expected as the previous results were taken using ambient condition AFM and STM with poorer tip quality and surface contamination issues.
(23) Michely, T.; Hohage, M.; Esch, S.; Comsa, G. *Surf. Sci.* **1996**, *349*, L89−L94.
(24) Islam, M. S.; Li, Z.; Ohlberg, D. A. A.; Stewart, D. R.; Chen, Y.; Wang, S. Y.; Williams, R. S. Unpublished results.
(25) Blackstock, J. J. Ph.D. Thesis, University of Alberta, 2004, in preparation.